Acta Crystallographica Section C
Crystal Structure Communications
ISSN 0108-2701

N-Methyl-*N*-phenylaminomethyl 2-naphthyl ketone: an X-ray diffraction and density functional theory study

Hasan Karabıyık,[a]* Sevnur Keskin,[b] Muhittin Aygün,[a] Nergis Arsu[b] and Orhan Büyükgüngör[c]

[a]Department of Physics, Dokuz Eylül University, 35160-Tınaztepe, İzmir, Turkey, [b]Department of Chemistry, Yıldız Technical University, 34210-Davutpaşa, İstanbul, Turkey, and [c]Department of Physics, Ondokuz Mayıs University, 55139-Kurupelit, Samsun, Turkey
Correspondence e-mail: hasan.karabiyik@deu.edu.tr

Received 28 December 2007
Accepted 31 January 2008
Online 16 February 2008

The crystallographically observed molecular structure of the title compound, $C_{19}H_{17}NO$, and its inverted counterpart are compared with that calculated by density functional theory (DFT) at the B3LYP/6-311++G(d,p) level. The results from both methods suggest that the observed molecular conformation of the title compound is primarily determined by intermolecular interactions in the crystal structure. The periodic organization of the molecules is stabilized by weak C—H···O and C—H···π hydrogen bonds and thus a two-dimensional puckered network consisting of $R_4^4(22)$ and $R_4^4(38)$ ring motifs is established. The title molecule has a (+)-antiperiplanar conformation about the C—C bond in the aminoacetone bridge. The pyramidal geometry observed around the vertex N atom is flattened by the presence of bulky phenyl and naphthylethanone fragments.

Comment

Considerable research effort has been devoted to the photo-initiated polymerization of acrylates and methacrylates due to their efficient usage for the rapid production of polymeric materials, in particular coatings and imaging materials, and photoresists for versatile applications (Pappas, 1978; Hageman, 1989; Dietliker, 1991; Fouassier, 1995; Davidson, 1999). Photoinitiators play an important role in UV-curable systems by generating the reactive species, free radicals or ions required to initiate the polymerization of multifunctional monomers and oligomers. We have recently synthesized 2-(*N*-methyl-*N*-phenylamino)acetonaphthone (MPA) (systematic name: *N*-methyl-*N*-phenylaminomethyl 2-naphthyl ketone), as a photoinitiator for the polymerization of methyl methacrylate (Keskin & Arsu, 2006). Since crystal structures of such materials are rare in the literature, our primary interest has been to understand their structural features in the solid state. To ascertain comprehensively the effects of crystallization on the isolated conformer of MPA, its solid-state structure was established by single-crystal X-ray diffraction analysis and compared with that optimized by density functional theory (DFT) calculation at the B3LYP/6-311++G(d,p) level (*GAUSSIAN03W*; Frisch *et al.*, 2004).

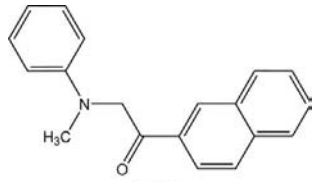

MPA

The molecular structure of MPA is shown in Fig. 1 and selected geometric parameters are listed in Table 1. The aminoacetone bridge [N—C(H$_2$)—C(=O)—C(Ar)] linking the naphthalene fragment with the phenyl ring is slightly distorted from its regular planar arrangement. The N1—C12—C11—C1 torsion angle is 174.8 (2)°, which shows that the conformation about the C12—C11 bond in the reference molecule is (+)-antiperiplanar. In the optimized geometry, the conformational descriptor around this torsion angle is also (+)-antiperiplanar, with a value of 173.29°. The bulky phenyl and naphthylethanone fragments on atom N1 favour a flattening of the pyramid-like geometry, resulting in the sum of the bond angles around the vertex atom (N1) being 358.2 (3)°. Methyl atom C13 deviates slightly from the plane defined by atoms C12, N1 and C14 by 0.34 (1) Å. In the optimized geometry, the corresponding deviation of the methyl C atom is a little smaller at 0.30 Å. Although the optimized geometric parameters are generally in agreement with those found in the crystal structure (Table 1), there are certain discrepancies between them, in particular the orientation of the naphthalene fragment. The structural discrepancies between the energy-minimized molecule and the crystallographically observed geometries (MPA itself and its inverted counterpart) were analysed quantitatively by r.m.s. overlays including the H atoms (Fig. 2). The r.m.s. fits of the atomic positions of MPA and its inverted counterpart to their corresponding values in the optimized geometry (Figs. 2*a* and 2*b*) are 0.0205 and 0.0698 Å, respectively. The r.m.s. fit of the atomic positions of MPA to those of its inverted counterpart (Fig. 2*c*) is 0.0596 Å.

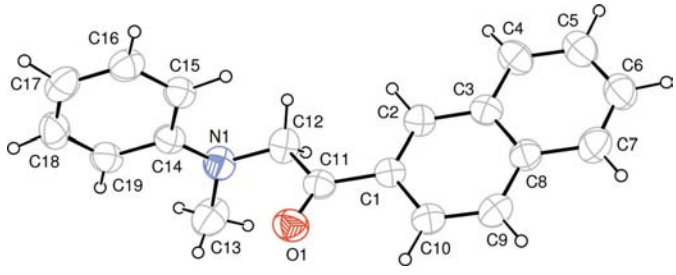

Figure 1
The molecule of the title compound, showing the atom-labelling scheme. Displacement ellipsoids are drawn at the 30% probability level and H atoms are shown as small spheres of arbitrary radii.

 doi:10.1107/S0108270108003466

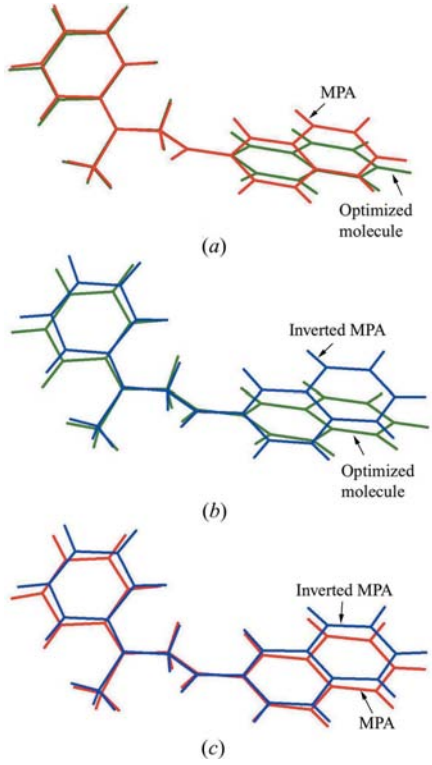

Figure 2
Superimpositions of (*a*) the reference molecule and the optimized geometry, (*b*) the inverted molecule and the optimized geometry and (*c*) the reference molecule and its symmetry-related inverse in the crystal structure.

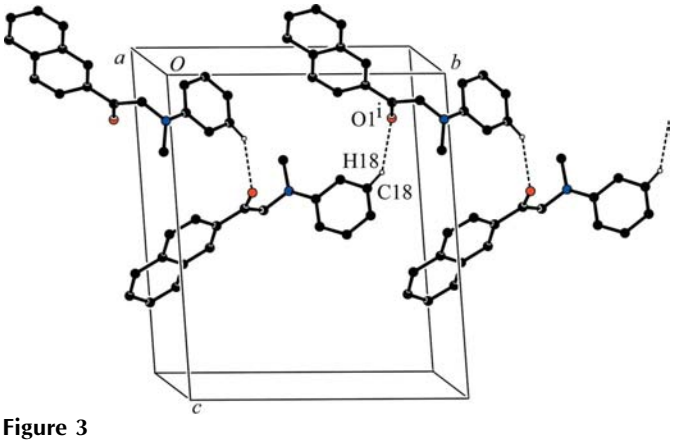

Figure 3
The hydrogen-bonded *C*(8) chain along the *b* axis of the unit cell. H atoms not involved in the motif shown have been omitted for the sake of clarity. [Symmetry code: (i) $-x, \frac{1}{2}+y, \frac{1}{2}-z$.]

While the dihedral angle between the phenyl and naphthalene fragments is 81.26 (7)° in MPA itself [−81.26 (7)° in the inverted molecule], this angle is 87.46° in the inverted optimized geometry. It can be inferred from these results that the conformations of MPA in the crystal structure and the free molecule are slightly different. These deformations in the crystallographically observed geometries of MPA are probably due to weak intermolecular interactions in the crystal lattice.

According to graph-set notation (Bernstein *et al.*, 1995), the molecules of MPA are linked into one-dimensional polymeric

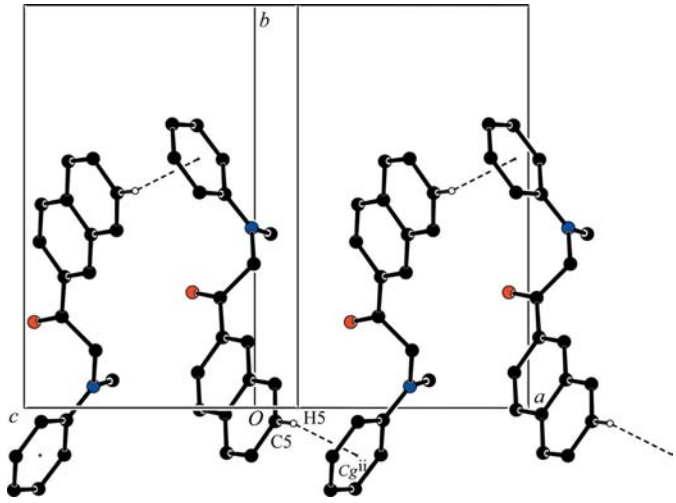

Figure 4
The formation of the chain along [201] generated by the C—H···π interaction. For the sake of clarity, H atoms not involved in the motif have been omitted. [Symmetry code: (ii) $1+x, \frac{1}{2}-y, \frac{1}{2}+z$.]

C(8) chains generated by a twofold screw operation parallel to the *b* axis of the unit cell *via* weak C18—H18···O1^{i} hydrogen bonds [symmetry code: (i) $-x, \frac{1}{2}+y, \frac{1}{2}-z$] (Fig. 3 and Table 2). On the other hand, there is a noteworthy C—H···π interaction (Fig. 4) in the crystal structure involving the C14–C19 phenyl ring (centroid *Cg*1) and atom C5 in the naphthalene fragment of a neighbouring molecule [C5—H5···*Cg*1^{ii}: H5···*Cg*1^{ii} = 2.70 Å and C5—H5···*Cg*1^{ii} = 154°; symmetry code: (ii) $1+x, \frac{1}{2}-y, \frac{1}{2}+z$]. This interaction forms a one-dimensional supramolecular arrangement running along the [201] direction, as shown in Fig. 4, involving both the reference molecules and their inverted counterparts consecutively.

The interactions mentioned above generate two different supramolecular arrangements. In the first, the acetonaphthone fragments of the molecules at (x, y, z) and $(1-x, -y, 1-z)$, together with the phenylamine fragments of the molecules at $(-x, y-\frac{1}{2}, \frac{1}{2}-z)$ and $(1+x, \frac{1}{2}-y, \frac{1}{2}+z)$, give rise to the formation of pseudocyclic centrosymmetric $R_4^4(22)$ synthons having their symmetry centre at $(\frac{1}{2}, 0, \frac{1}{2})$, as shown in Fig. 5. Propagation of the first supramolecular arrangement by the space-group-symmetry operations links the $R_4^4(22)$ synthon centred at $(\frac{1}{2}, 0, \frac{1}{2})$ to the next one centred at $(\frac{1}{2}, 1, \frac{1}{2})$, so generating the second supramolecular arrangement as a pseudocyclic centrosymmetric $R_4^4(38)$ ring having its symmetry centre at $(\frac{1}{2}, \frac{1}{2}, \frac{1}{2})$ (Fig. 5). Thus, a rather complex puckered sheet lying almost parallel to $(10\bar{2})$ is formed by these supramolecular units.

In order to investigate quantitatively the possible effects of the intermolecular interactions on the aromaticity of the naphthalene fragment, HOMA (harmonic oscillator model of aromaticity) indices (Krygowski, 1993) were calculated for the crystallographic and optimized geometry of MPA. The HOMA index is equal to unity for purely aromatic systems and zero for non-aromatic systems. The calculated HOMA indices for the naphthalene fragment of the crystallographically observed and optimized geometries of MPA are 0.849 and 0.811, respectively. On the other hand, the HOMA

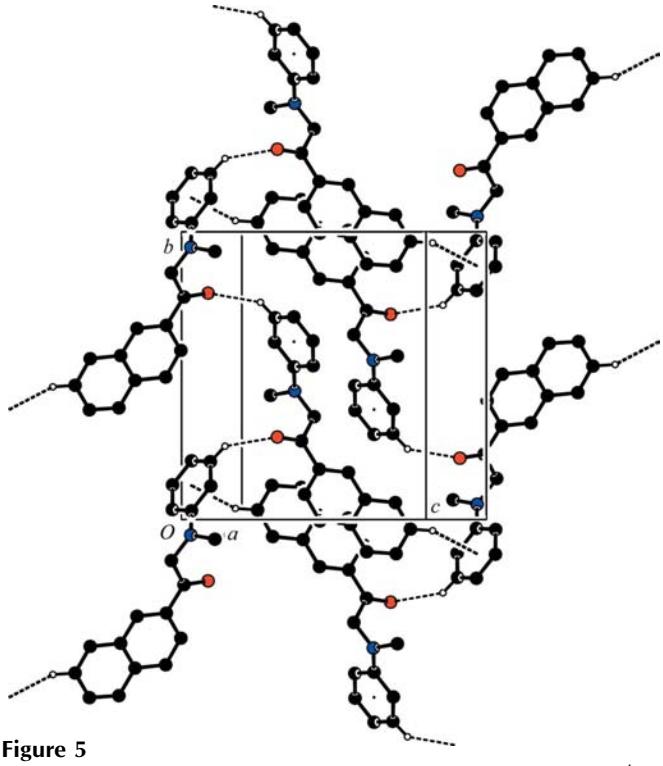

Figure 5
Part of the crystal structure of MPA, showing the formation of the $R_4^4(22)$ and $R_4^4(38)$ ring motifs.

index for naphthalene is 0.81 (Krygowski, 1993) and this value may vary from 0.810 to 0.854 depending on the experimental quality (Rosokha & Kochi, 2006). It can be stated that the intermolecular interactions have a restricted effect on the covalent topology of the naphthalene fragment, but a remarkable effect on its orientation.

Experimental

The synthesis of MPA and the corresponding spectroscopic data have already been reported by Keskin & Arsu (2006).

Crystal data

$C_{19}H_{17}NO$
M_r = 275.34
Monoclinic, $P2_1/c$
a = 8.6049 (8) Å
b = 12.6787 (7) Å
c = 15.5042 (14) Å
β = 117.900 (6)°
V = 1494.9 (2) Å^3
Z = 4
Mo $K\alpha$ radiation
μ = 0.07 mm^{-1}
T = 296 (2) K
0.42 × 0.34 × 0.26 mm

Data collection

Stoe IPDSII diffractometer
22658 measured reflections
2182 independent reflections
1219 reflections with $I > 2\sigma(I)$
R_{int} = 0.096

Refinement

$R[F^2 > 2\sigma(F^2)]$ = 0.054
$wR(F^2)$ = 0.133
S = 1.04
2182 reflections
190 parameters
6 restraints
H-atom parameters constrained
$\Delta\rho_{max}$ = 0.12 e Å^{-3}
$\Delta\rho_{min}$ = −0.12 e Å^{-3}

The crystallographically observed geometry of MPA was chosen as the starting geometry in the optimization procedure. Geometry optimization and vibrational analysis were performed without any constraints on the molecule using the B3LYP hybrid exchange-correlation function (Stephens *et al.*, 1994) with the aid of the 6-311++G(d,p) basis set. All normal frequencies at the optimized geometry are real, showing that the optimization results in a stable minimum. All calculations were carried out using *GAUSSIAN03W* (Frisch *et al.*, 2004). All H atoms were located in their idealized positions and refined using suitable riding models, with C—H distances in the range 0.93–0.97 Å and with U_{iso}(H) values of $1.2U_{eq}$(C) or $1.5U_{eq}$(methyl C). Following refinement, the anisotropic displacement parameters of atoms C17 and C18 were restrained to be similar (SIMU instruction in *SHELXL97*; Sheldrick, 2008). The crystal sample selected for data collection was nonmerohedrally twinned (twin lattice quasi-crystal, TLQS) by a twofold rotation axis perpendicular to (010) with two reciprocal lattices differently oriented, giving rise to double diffraction spot sets (see supplementary material) with a twinning ratio of 0.51:0.49. We were aware of the twin character of the crystal samples at the data collection stage, but pure crystals having a single diffraction spot set could not be found. Since the partially overlapped reflections arising from the nonmerohedral character of the crystal sample could not be integrated separately, 752 partially overlapped independent reflections could not be measured satisfactorily and they were discarded from the data set. As a result, the completeness of the data decreased to slightly over 74%.

Data collection: *X-AREA* (Stoe & Cie, 2002); cell refinement: *X-AREA*; data reduction: *X-RED* (Stoe & Cie, 2002); program(s) used to solve structure: *SHELXS97* (Sheldrick, 2008); program(s) used to refine structure: *SHELXL97* (Sheldrick, 2008); molecular graphics: *PLATON* (Spek, 2003) and *ORTEP-3* (Farrugia, 1997); software used to prepare material for publication: *WinGX* (Farrugia, 1999) and *enCIFer* (Allen *et al.*, 2004).

Table 1
Hydrogen-bond geometry (Å, °).

D—H···A	D—H	H···A	D···A	D—H···A
C18—H18···O1^{i}	0.93	2.60	3.341 (4)	137

Symmetry code: (i) $-x, y+\frac{1}{2}, -z+\frac{1}{2}$.

Table 2
Comparison of selected geometric parameters of MPA (Å, °) from X-ray diffraction and DFT studies.

	X-ray	DFT/B3LYP
C14—N1	1.384 (4)	1.396
N1—C12	1.433 (4)	1.442
C12—C11	1.524 (4)	1.544
C11—O1	1.216 (3)	1.221
C11—C1	1.483 (4)	1.497
N1—C13	1.451 (4)	1.457
C14—N1—C12	122.0 (2)	120.48
N1—C12—C11	115.0 (2)	114.72
O1—C11—C12	120.3 (3)	119.94
C1—C11—C12	118.0 (3)	119.00
C2—C1—C11—O1	−167.6 (3)	−178.54
O1—C11—C12—N1	−3.9 (4)	−4.77
C15—C14—N1—C13	167.0 (3)	167.66
C10—C1—C11—O1	13.0 (4)	1.22
C15—C14—N1—C12	2.6 (4)	7.93
C2—C1—C11—C12	13.8 (4)	0.32

The authors thank Dokuz Eylül, Yıdız Technical and Ondokuz Mayıs University Research Funds (respective project Nos. 04.KB.FEN.100, 20-0-02-02 and F.279) for financial support of this work. In addition, HK thanks TÜBİTAK (the Scientific and Technical Research Council of Turkey) for partial financial support.

Supplementary data for this paper are available from the IUCr electronic archives (Reference: LN3084). Services for accessing these data are described at the back of the journal.

References

Allen, F. H., Johnson, O., Shields, G. P., Smith, B. R. & Towler, M. (2004). *J. Appl. Cryst.* **37**, 335–338.
Bernstein, J., Davis, R. E., Shimoni, L. & Chang, N.-L. (1995). *Angew. Chem. Int. Ed. Engl.* **34**, 1555–1573.
Davidson, R. S. (1999). *Exploring the Science, Technology and Applications of UV and EB Curing*, pp. 80–84. London: SITA Technology Ltd.
Dietliker, K. (1991). *Chemistry and Technology of UV and EB Formulation for Coatings, Inks and Paints*, Vol. 3, pp. 76–78. London: SITA Technology Ltd.
Farrugia, L. J. (1997). *J. Appl. Cryst.* **30**, 565.
Farrugia, L. J. (1999). *J. Appl. Cryst.* **32**, 837–838.
Fouassier, J.-P. (1995). *Photoinitiation, Photopolymerization and Photocuring: Fundamentals and Applications*, pp. 1-7. Munich: Hanser Verlag.
Frisch, M. J. *et al.* (2004). *GAUSSIAN03W*. Revision C.02. Gaussian Inc., Wallingford, Connecticut, USA.
Hageman, H. S. (1989). *Photopolymerization and Photoimaging Science and Technology*, edited by N. S. Allen, pp. 1–53. London: Elsevier.
Keskin, S. & Arsu, N. (2006). *Polym. Bull.* **57**, 643–650.
Krygowski, T. M. (1993). *J. Chem. Inf. Comput. Sci.* **33**, 70–78.
Pappas, S. P. (1978). *UV Curing Science and Technology*, pp. 2–13. Norwalk, Connecticut: Technology Marketing Corporation.
Rosokha, S. V. & Kochi, J. K. (2006). *J. Org. Chem.* **71**, 9357–9365.
Sheldrick, G. M. (2008). *Acta Cryst.* A**64**, 112–122.
Spek, A. L. (2003). *J. Appl. Cryst.* **36**, 7–13.
Stephens, P. J., Devlin, F. J., Chablowski, C. F. & Frisch, M. J. (1994). *J. Phys. Chem.* **98**, 11623–11627.
Stoe & Cie (2002). *X-AREA* (Version 1.18) and *X-RED32* (Version 1.04). Stoe & Cie, Darmstadt, Germany.